Excitation-induced dephasing and ultrafast intrasubband relaxation in carbon nanotubes

Matthias Hirtschulz, Ermin Malic,* Frank Milde, and Andreas Knorr
Institut für Theoretische Physik, Technische Universität Berlin, 10623 Berlin, Germany
(Received 22 April 2009; published 5 August 2009)

We present theoretical investigations of the ultrafast relaxation dynamics and the excitation-induced dephasing of excitonic polarization in single-walled carbon nanotubes. Our microscopic approach is based on the density-matrix theory combined with tight-binding wave functions allowing the calculation of tubes with arbitrary diameter and chiral angle. For excitations to the single-particle continuum, the initial nonequilibrium carrier distribution is thermalized within approximately 100 fs while the polarization adiabatically follows the excitation pulse. For excitations at the excitonic resonance, we find a dephasing of the excitonic polarization on a picosecond time scale depending on the excitation strength. With increasing field intensities, the dephasing time linearly decreases, which is in agreement with recent experiments.

DOI: 10.1103/PhysRevB.80.085405 PACS number(s): 73.22.−f, 78.47.J−, 78.67.Ch, 42.65.−k

I. INTRODUCTION

During the last years, the electronic and optical properties of single-walled carbon nanotubes (CNTs) have been studied intensively due to their promising potential applications in various areas.[1,2] Recently, also nonlinear and ultrafast optical properties of CNTs became accessible in experimental studies.[3,4] In particular, pump-probe and four-wave mixing experiments allow the determination of intrinsic lifetimes and related scattering mechanisms in these quasi-one-dimensional structures. The theoretical understanding and modeling of these phenomena has been limited to very few calculations so far.[5–7] In this work, we present an approach, which combines the density-matrix theory for investigating the dynamics with the tight-binding approximation for calculating the band structure of CNTs.[8] It allows the investigation of both linear and nonlinear response to optical pulses taking into account many-particle interactions. This way, CNTs of different diameter and chirality can be analyzed within acceptable computation time. To describe ultrafast carrier relaxation a mean-field theory is not sufficient. Hence, the Hartree-Fock description presented in Ref. 8 must be extended to be able to include carrier-carrier interaction for intraband equilibration of optically detected carriers as well as the dephasing of the optically induced polarization.[7] The aim of this work is a comprehensive microscopic description of the ultrafast relaxation and the optical dephasing in CNTs by analyzing the influence of the carrier-carrier Coulomb interaction on these processes. To accurately describe carrier dynamics on very short-time scales below 100 fs a *non-Markovian theory* is necessary.[9] Therefore, a correlation expansion[10] was performed to account for carrier-carrier-interaction-induced memory effects, which act on short-time scales in the femtosecond regime. Here, we improve the model for the intraband relaxation presented in Ref. 7 to include both valence and conduction bands. The novel two-band calculations support the intrasubband carrier relaxation on a time scale of hundreds of femtoseconds previously obtained from the one-band calculations but also provide a detailed understanding of excitation-induced dephasing of the optical polarization. Excitonic effects shown to be of crucial importance for CNTs (Refs. 11 and 12) are fully taken into account. In particular, *excitation-induced dephasing* of the excitonic polarization occurs on a picosecond time scale depending on the carrier densities.

II. DENSITY MATRIX THEORY FOR CNTS

Our theoretical approach presented in Ref. 7 is extended to include excitons and to account for the optical excitation of carriers. Two bands, the conduction band $\lambda=c$ and the valence band $\lambda=v$ are considered. The Hamilton operator $H=H_f+H_C$ of the system consists of a free contribution H_f and a many-particle Coulomb interaction part H_C. H_f includes the single-particle band structure, i.e., the interaction of the electrons with the CNT lattice potential and with the external light field. The field is described by a linearly polarized vector potential parallel to the CNT axis having a Gaussian pulse envelope in temporal domain. As a result, the field can be described by the scalar $A(t)=A_0(t)(e^{i\omega_L t}+e^{-i\omega_L t})$ with the pulse envelope $A_0(t)=A_0 e^{-t^2/2\sigma^2}$. Within the formalism of the second quantization, single and many-particle operators can be written in terms of the creation $a^\dagger_{\lambda k}$ and annihilation operators $a_{\lambda k}$. These create (destroy) single-particle states $|\lambda k\rangle$ with band λ and linear momentum $\hbar k$. These single-particle states are treated within the tight-binding approximation.[8,13] The subband index for the conduction and valence bands is omitted throughout this work since we focus the description on a two-band model for CNTs. This is a well-defined approximation since we restrict the treatment to excitation energies $\hbar\omega_L$ near the lowest resonance E_{11}. The free part of the Hamilton operator finally reads

$$H_f=\sum_{\lambda=v,c}\sum_k E^\lambda_k a^\dagger_{\lambda k}a_{\lambda k}-\frac{\hbar}{i}\sum_k \Omega_k a^\dagger_{vk}a_{ck}+\text{c.c.} \qquad (1)$$

Here, $E^\lambda(k)$ is the single-particle tight-binding energy[7,8] and Ω_k is the Rabi frequency $\Omega_k=\frac{e_0}{m_0}M^{vc}_k A(t)$. m_0 is the free-electron mass, e_0 is the electron charge, and $M^{vc}_k=\langle vk|\nabla|ck\rangle$ are the optical matrix elements.[14,15] The second part of the Hamilton operator H_C describes the Coulomb interaction of the carriers in CNT

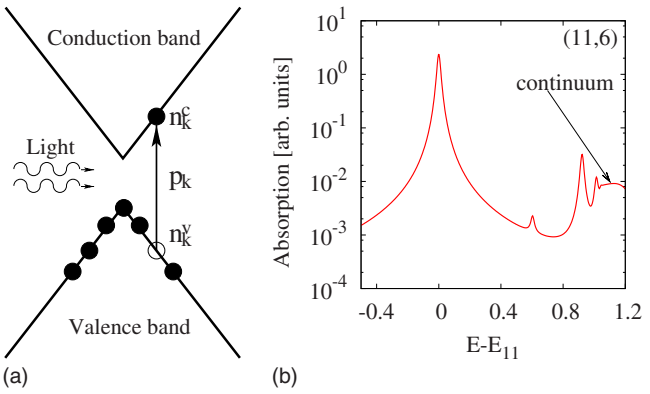

FIG. 1. (Color online) (a) Schematic illustration of microscopic polarization $p_k(t)$ and occupation densities $n_k^c(t)$ and $n_k^c(t)$ (b) absorption spectrum of a (11,6) CNT (logarithmic scale). The lowest excitonic resonance at $E=E_{11}=0.94$ eV is followed by higher excitonic resonances and the single-particle continuum at $E-E_{11}=1.04$ eV(arrow). Hence, an excitation at $\hbar\omega_L=2.01$ eV corresponds to an excess energy of 24 meV above the renormalized band edge.

$$H_C = \frac{1}{2}\sum_{\lambda_1,\ldots,\lambda_4}\sum_{k,q,k'} V^{\lambda_1\lambda_2\lambda_3\lambda_4}_{(k,q,k')} a^\dagger_{\lambda_1 k+q} a^\dagger_{\lambda_2 k'} a_{\lambda_4 k'+q} a_{\lambda_3 k} \quad (2)$$

with Coulomb matrix elements $V^{\lambda_1\lambda_2\lambda_3\lambda_4}_{(k,q,k')} \equiv \langle \lambda_1 k+q|\langle \lambda_2 k'|V(\mathbf{r}-\mathbf{r}')|\lambda_3 k\rangle|\lambda_4 k'+q\rangle$ and the regularized Coulomb potential[8] $V(\mathbf{r}-\mathbf{r}')$. Throughout this work, quantities with four indices such as the Coulomb matrix elements of the correlations are abbreviated as $X^{\lambda_1\lambda_2\lambda_3\lambda_4}_{(k,q,k')} = X^{\lambda_1 k+q,\lambda_2 k'}_{\lambda_3 k,\lambda_4 k'+q}$.

The core of the density-matrix approach is to determine the dynamics of the one-particle density matrix. For a spatially homogeneous carrier system the elements of the one-particle density matrix $f_{12} \equiv \langle a_1^\dagger a_2\rangle$ (quantum numbers $1,\ldots,4$ are generic) are the microscopic polarization $p_k(t) \equiv \langle a_{vk}^\dagger a_{ck}\rangle$ and the electron populations $n_k^\lambda(t) \equiv \langle a_{\lambda k}^\dagger a_{\lambda k}\rangle$. $p_k(t)$ describes the transition between the valence and the conduction bands at the wave number k. Figure 1(a) illustrates the two-band CNT model. Via the Heisenberg equation of motion $\langle \dot{O}\rangle = \frac{i}{\hbar}\langle [H,O]\rangle$ we can determine the dynamics of the respective microscopic quantities. The expectation value is obtained from the density matrix ρ: $\langle O\rangle = \mathrm{Tr}\{O\rho\}$. In this way, one obtains equations of motion (EOM) for electronic occupations n_k^c and n_k^v and for the microscopic polarization p_k. The Coulomb contribution, however, couples the one-particle density matrix (singlets) to two-particle density matrices (doublets) $S_{34}^{12} \equiv \langle a_1^\dagger a_2^\dagger a_3 a_4\rangle$. This coupling to higher order density matrices is a result of Coulomb interaction being a many-particle interaction.[16] It introduces additional dynamic variables to the system of equations that have to be determined. The dynamics of the doublets S_{34}^{12} couples to three-particle quantities $Q_{456}^{123} \equiv \langle a_1^\dagger a_2^\dagger a_3^\dagger a_4 a_5 a_6\rangle$. This is the start of an infinite hierarchy of equations of motion that has to be truncated in a defined way. A systematic way to perform this truncation is the correlation expansion. In this approach, the two-particle density matrix S_{34}^{12} is split up into a mean field and a correlation contribution C_{34}^{12}: $S_{34}^{12} = f_{14}f_{23} - f_{13}f_{24} + C_{34}^{12}$, similar equations are valid for Q_{456}^{123}. In this way the correlations are a measure of the deviations from the mean-field description. They can be divided into coherent and incoherent correlations depending on their decay times[17] (see below). On the level of the two-particle correlation we truncate the hierarchy of EOM and neglect the three-particle correlations. Next we discuss the details of the EOM for (a) the polarization $p_k(t)$, (b) the occupation $n_k^\lambda(t)$, and (c) the correlations C_{34}^{12}.

(a) Polarization dynamics. The dynamics of the optical polarization $p_k(t)$ is driven by the coherent classical field, the Hartree-Fock contributions, and the *coherent* correlations $\dot{p}_k|_{co}$ that lead to effects such as excitation-induced dephasing[17] of the polarization. In rotating wave approximation,[8] we have

$$\dot{p}_k = i(\omega_L - \tilde{\omega}_k^{cv})p_k - \tilde{\Omega}_k(t)(n_k^v - n_k^c) + \dot{p}_k|_{co} \quad (3)$$

with $\tilde{\omega}_k^{cv} = (\tilde{E}_k^c - \tilde{E}_k^v)/\hbar$ being the renormalized band gap. The renormalization of the electronic dispersion arises from the Hartree-Fock contributions of the Coulomb interaction $\tilde{E}_k^\lambda = E_k^\lambda - \Sigma_{\lambda',q} V^{\lambda'\lambda\lambda\lambda'}_{(k,q,k)} n^{\lambda'}_{k+q}$ and causes strong shifts and modification of the CNT single-particle band dispersion. $\tilde{\Omega}(t)$ is the renormalized Rabi frequency

$$\tilde{\Omega}_k = \frac{e_0}{m} M_k^{vc} A_0(t) - \frac{i}{\hbar}\sum_{q\neq 0} V^{vcvc}_{(k,q,k)} p_{k+q}. \quad (4)$$

The renormalization of the external field $A_0(t)$ is caused by excitonic Hartree-Fock contributions. This renormalization leads to excitonic resonances of the system.[8] The third term in Eq. (3) is the correlation contribution to the polarization dynamics. It couples the microscopic polarization $p_k(t)$ to the coherent doublet correlations $C^{\lambda_1\lambda_2\lambda_3\lambda_4}_{(k,q,k')}$,

$$\begin{aligned}\dot{p}_k|_{co} = \frac{i}{\hbar}\sum_{q,k'} [& V^{cccc}_{(k',q,k)} C^{cvcc}_{(k',q,k)} + V^{vcvc}_{(k',q,k)} C^{vvvc}_{(k',q,k)} \\ & + V^{vccv}_{(k',q,k)} C^{vvvc}_{(k+q,-q,k'+q)} - V^{vcvc}_{(k,q,k')} C^{cvcc}_{(k'+q,-q,k+q)} \\ & - V^{cvvc}_{(k,q,k')} C^{cvcc}_{(k,q,k')} - V^{vvvv}_{(k,q,k')} C^{vvvc}_{(k'+q,-q,k+q)}].\end{aligned} \quad (5)$$

(b) Occupation density dynamics. The dynamics of the conduction-band and valence-band electron densities n_k^c and n_k^v are determined by the exciting pulse and (in contrast to the coherence p_k) by *incoherent* correlations $\dot{n}_k^\lambda|_{co}$,

$$\dot{n}_k^c = 2\,\mathrm{Re}\{\tilde{\Omega}_k^*(t)p_k(t)\} + \dot{n}_k^\lambda|_{co}. \quad (6)$$

The last term in Eq. (6) $\dot{n}_k^\lambda|_{co}$ describes the coupling of the occupation densities to the two-particle density matrix

$$\begin{aligned}\dot{n}_k^\lambda|_{co} = \frac{2}{\hbar}\mathrm{Im}\Big[\sum_{k',q} & V^{cccc}_{(k,q,k')} C^{cccc}_{(k,q,k')} + V^{cvcv}_{(k,q,k')} C^{cvcv}_{(k,q,k')} \\ & + V^{vccv}_{(k,q,k')} C^{vccv}_{(k,q,k')}\Big].\end{aligned} \quad (7)$$

Within the present tight-binding approximation of the single-particle band structure (neglecting overlaps integrals s_0 between nearest neighbors) valence and conduction bands are

symmetric ($\omega_k^c=-\omega_k^v$) and the corresponding dynamics of the valence-band densities can be obtained via $\dot{n}_k^c=-\dot{n}_k^v$. As shown later (Sec. III) the dynamics of the correlations appearing in Eq. (6) describes the redistribution of carriers within the subbands via Coulomb scattering. The dynamics of the correlations appearing in Eqs. (3) and (6) are obtained from the correlation expansion.

(c) Correlation dynamics. The dynamics of the doublet correlations C_{34}^{12} [cp. Eqs. (3) and (6)] is driven by the single-particle scattering contributions treated equivalently to a second-order Born description. However, since one keeps the full time dynamics without applying a Markovian approximation, they contain the memory of the many-particle interaction. Additional electron-light coupling terms in the correlation dynamics are neglected since they are of higher order in the field than the correlations itself. We performed calculations including these terms to verify this argument showing no significant difference. As an example, we present the dynamics of the incoherent carrier-carrier correlation $C_{(k,q,k')}^{cccc}$ and the coherent electron-assisted polarization $C_{(k,q,k')}^{cvcc}$. The dynamics of all other correlations can be obtained by symmetry arguments.[17] The incoherent correlations are driven by singlet contributions even when no polarizations are present in the system (incoherent regime). The carrier-carrier correlation $C_{(k,q,k')}^{cccc}$ describes the scattering between carriers in the conduction band,

$$\begin{aligned}\frac{\hbar}{i}\dot{C}_{(k,q,k')}^{cccc} &= \hbar(\omega_{k+q}^c+\omega_{k'}^c-\omega_k^c-\omega_{k'+q}^c)C_{(k,q,k')}^{cccc}-W_{(k',q,k)}^{vcvc}\\ &\times[(n_{k'}^c-n_{k'+q}^c)p_k p_{k+q}^*+(n_{k+q}^c-n_k^c)p_{k'+q}p_{k'}^*]\\ &-W_{(k',q,k)}^{vccv}[(n_{k'}^c-n_k^c)p_{k'+q}p_{k+q}^*+(n_{k+q}^c\\ &-n_{k'+q}^c)p_k p_{k'}^*]-W_{(k',q,k)}^{cccc}[(1-n_{k+q}^c-n_{k'}^c)n_k^c n_{k'+q}^c\\ &-(1-n_k^c-n_{k'+q}^c)n_{k+q}^c n_{k'}^c], \end{aligned} \tag{8}$$

where $W_{(k',q,k)}^{\lambda_1\lambda_2\lambda_3\lambda_4}=V_{(k',q,k)}^{\lambda_1\lambda_2\lambda_3\lambda_4}-V_{(k',k-k',k'+q)}^{\lambda_2\lambda_1\lambda_3\lambda_4}$. In contrast to the incoherent correlation, the coherent correlations are only driven as long as the polarizations $p_k(t)$ have not been decayed. In the fully incoherent limit they are not driven via singlet contributions,

$$\begin{aligned}\frac{\hbar}{i}\dot{C}_{(k,q,k')}^{cvcc} &= \hbar(\omega_{k+q}^c+\omega_{k'}^v-\omega_k^c-\omega_{k'+q}^c+\omega_L)C_{(k,q,k')}^{cvcc}\\ &-W_{(k',q,k)}^{vcvc}[n_{k+q}^c n_{k'}^v p_{k'+q}+p_{k'}p_k p_{k+q}^*+(1-n_{k+q}^c\\ &-n_{k'}^v)n_k^c p_{k'+q}]-W_{(k',q,k)}^{vccv}[n_{k+q}^c n_{k'}^v p_k+p_{k'}p_{k'+q}p_{k+q}^*\\ &+(1-n_{k+q}^c-n_{k'}^v)n_{k'+q}^c p_k]+W_{(k',q,k)}^{cccc}[n_k^c n_{k'+q}^c p_{k'}\\ &+p_k p_{k'+q}p_{k+q}^*+(1-n_k^c-n_{k'+q}^c)n_{k+q}^c p_{k'}]. \end{aligned} \tag{9}$$

III. RELAXATION DYNAMICS

Evaluating the equations of motion for the microscopic polarization $p_k(t)$ in the linear optical regime[8] one obtains the linear absorption, see Fig. 1(b). The excitonic resonance at $E_{11}=0.94$ eV and the renormalized band edge at 1.99 eV characterize the system. Here, we show the results for an exemplary chiral tube, namely (11,6) CNT. The numerical evaluation of Eqs. (3) and (6) beyond the linear regime yields insight into the intrasubband relaxation dynamics as well as into the optical dephasing.

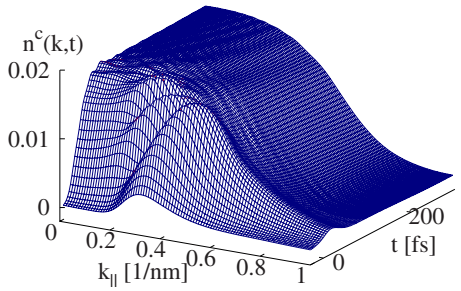

FIG. 2. (Color online) Carrier dynamics $n_k^c(t)$ for excitation located above the renormalized band edge. The carriers relax from their initial nonequilibrium distribution into a Fermi-type distribution after around 100 fs.

First, we present a calculation of the *intrasubband relaxation* for excitation above the renormalized band edge, i.e., carriers are excited to the single-particle continuum depicted in Fig. 1(b). In Fig. 2, the carrier dynamics is shown as a function of wave number and time after the peak of input pulse at $t=0$ for $A_0=0.13\frac{\text{eV fs}}{e_0\cdot\text{nm}}$ and $\sigma=28$ fs). The excitation is energetically located at $\hbar\omega_L=2.01$ eV (corresponding to an excess energy of 24 meV) far above the excitonic resonance at 0.942 eV. This pulse excites a collection of single-particle states with maximum occupation density at around $k_\parallel\approx 0.5/\text{nm}$ $(t=0)$. Later on $(t>0)$ oscillations of the electron plasma set in with a period of around 16 fs. They are a result of the non-Markovian dynamics. The carriers equilibrate into a Fermi-type distribution within approximately $\lesssim$100 fs. For these excitation conditions the total polarization $P(t)=\frac{1}{L}\Sigma_k p_k$ adiabatically follows the pulse with a delay of about 5 fs (Fig. 3). This behavior occurs due to the continuum excitation, where rapid interference of single-particle states and carrier-scattering-induced dephasing slaves the polarization to the field dynamics. In contrast to the rapidly

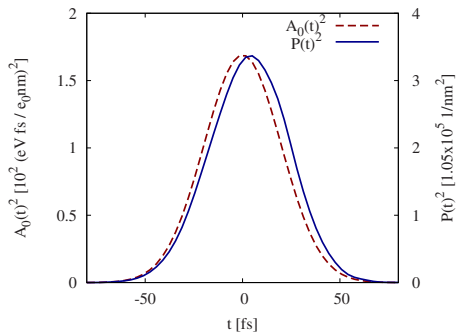

FIG. 3. (Color online) The pulse envelope $A_0(t)^2$ in comparison with the dynamics of the absolute square of the total polarization $|P(t)|^2$ (normalized to maximum field intensity). The polarization adiabatically follows the pump pulse with a small time delay.

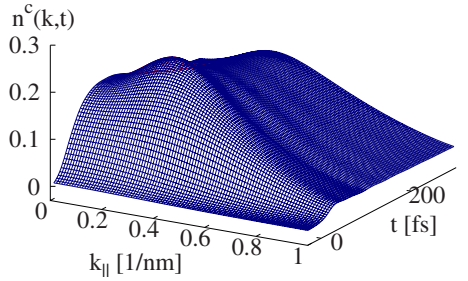

FIG. 4. (Color online) Carrier dynamics $n_k^c(t)$ for excitation located at the excitonic resonance. The excitation of carrier occupation densities represents the correlated many-particle excitonic state in a single-particle basis.

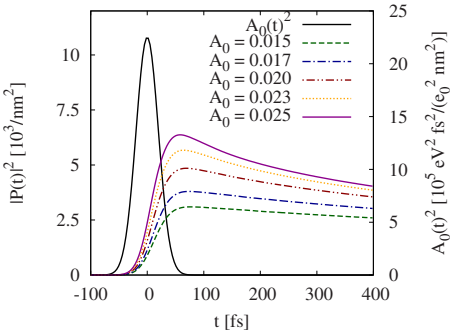

FIG. 5. (Color online) Total polarization $|P(t)|^2$ after resonant excitation of a (11,6) CNT with different excitation amplitudes A_0 $[A_0=(0.015-0.025)\frac{\text{eV fs}}{e_0\cdot\text{nm}}$, $\sigma=28$ fs]. After the pulse has vanished the total polarization decays on a picosecond time scale. With increasing excitation amplitude (higher carrier density) the dephasing rate increases. This is because the effect of excitation-induced dephasing increases with higher occupation densities.

vanishing polarization, the carriers remain in the system (cp. Fig. 2). In a more detailed theory, valid on a picosecond to nanosecond times scale, the occupations relax back to the valence band, e.g., via radiative decay not included in this model.

Second, we focus on excitation at the exciton resonance. The corresponding carrier dynamics $n_k^c(t)$ is shown in Fig. 4. Note that the carrier occupation is one order of magnitude higher than in the on-resonant case, which can be ascribed to the much stronger excitonic oscillator strength. At these excitation conditions, excitonic correlated states are excited. Therefore, one does not observe comparable plasmonic oscillations comparable to the band-edge excitation in Fig. 2. For strong enough excitation, the carrier occupations and polarizations induce the interference of different correlations that lead to a dephasing of the excitonic polarization in dependence of the number of scattering carriers, which are optically excited. This effect is called *polarization-induced dephasing*.[17,18] To discuss this effect for CNTs, we have done calculations for resonant excitation at the excitonic resonance [(11,6) CNT, $\Delta=0$, and $\sigma=28$ fs] for different amplitudes $A_0=0.015\frac{\text{eV fs}}{e_0\cdot\text{nm}}$ up to $A_0=0.025\frac{\text{eV fs}}{e_0\cdot\text{nm}}$ to examine the influence of excitation on the optical dephasing at the excitonic resonance.[19]

Figure 5 shows the polarization dynamics $|P(t)|^2$ for different amplitudes of the pulse A_0. In contrast to excitation at the band edge, the polarization does not adiabatically follow the optical pulse. This is due to the excitation of a bound state (exciton) below the carriers continuum, thus suppressing simple single-particle interference effects. With larger pulse amplitudes, the induced polarization is increased and at the same time the dephasing rate (polarization decay) is linearly increased. This behavior is a consequence of the larger occupation densities for stronger field amplitudes leading to more scattering partners in the conduction band. As a result, the dephasing of the excitonic polarization is accelerated. This trend is consistent with recent experimental findings.[4] For the excitation conditions considered here, an excitation-dependent dephasing of the polarization on a picosecond time scale is found.

IV. CONCLUSIONS

In summary, we have developed a two-band model combining density-matrix theory and tight-binding wave functions to describe ultrafast phenomena in arbitrary single-wall carbon nanotubes. We have demonstrated the ability of the approach to describe Coulomb quantum kinetics and excitation-induced dephasing on an ultrashort time scale. Including the many-particle Coulomb interaction beyond the Markov approximation allows the description of memory effects that are important on the femtosecond time scale. We have done exemplary calculations for the (11,6) single-wall carbon nanotube, however, the approach can be applied for tubes with arbitrary chiral angle and diameter (within the restriction of the tight-binding model). One obtains an ultrafast carrier relaxation on a femtosecond time scale, when the CNT is excited by an ultrashort pump pulse. For excitation at the excitonic resonance, we find an excitation-induced dephasing of the total polarization on a picosecond time scale. With increasing excitation intensity the Coulomb-scattering-induced dephasing increases. This trend is in line with recent experimental findings.[4] To further improve the theory, excitonic like Coulomb correlation contributions as well as electron-phonon (polaron) interaction can be included similar to Refs. 6, 16, and 20–23.

ACKNOWLEDGMENTS

Support from the Cluster of Excellence "Unifying Concepts in Catalysis" (DFG) and Sfb 658 "Elementary Processes in Molecular Switches at Surfaces" are acknowledged.

*ermin@itp.physik.tu-berlin.de

[1] S. Reich, C. Thomsen, J. Maultzsch, and M. Janina, *Carbon Nanotubes: Basic Concepts and Physical Properties* (Wiley-VCH, Berlin, 2004).
[2] A. Jorio and M. Dresselhaus, *Carbon Nanotubes: Advanced Topics in the Synthesis, Structure, Properties and Applications* (Springer, New York, 2008).
[3] A. Hagen, G. Moos, V. Talalaev, and T. Hertel, Appl. Phys. A: Mater. Sci. Process. **78**, 1137 (2004).
[4] Y. Ma, M. Graham, G. Fleming, A. Green, and M. Hersam, Phys. Rev. Lett. **101**, 217402 (2008).
[5] B. F. Habenicht, C. F. Craig, and O. V. Prezhdo, Phys. Rev. Lett. **96**, 187401 (2006).
[6] S. Butscher and A. Knorr, Phys. Rev. Lett. **97**, 197401 (2006).
[7] M. Hirtschulz, F. Milde, E. Malic, C. Thomsen, S. Reich, and A. Knorr, Phys. Status Solidi B **245**, 2164 (2008).
[8] M. Hirtschulz, F. Milde, E. Malić, S. Butscher, C. Thomsen, S. Reich, and A. Knorr, Phys. Rev. B **77**, 035403 (2008).
[9] H. Haug and A. Jauho, *Quantum Kinetics in Transport and Optics of Semiconductors* (Springer Verlag, Berlin, 2007).
[10] H. Haug and S. Koch, *Quantum Theory of the Optical and Electronic Properties of Semiconductors* (World Scientific, Singapore, 2004).
[11] F. Wang, G. Dukovic, L. E. Brus, and T. F. Heinz, Science **308**, 838 (2005).
[12] J. Maultzsch, R. Pomraenke, S. Reich, E. Chang, D. Prezzi, A. Ruini, E. Molinari, M. S. Strano, C. Thomsen, and C. Lienau, Phys. Rev. B **72**, 241402(R) (2005).
[13] R. Saito, G. Dresselhaus, and M. Dresselhaus, *Physical Properties of Carbon Nanotubes* (World Scientific, Singapore, 2003).
[14] A. Grüneis, R. Saito, G. G. Samsonidze, T. Kimura, M. A. Pimenta, A. Jorio, A. G. Souza Filho, G. Dresselhaus, and M. S. Dresselhaus, Phys. Rev. B **67**, 165402 (2003).
[15] E. Malić, M. Hirtschulz, F. Milde, A. Knorr, and S. Reich, Phys. Rev. B **74**, 195431 (2006).
[16] M. Lindberg and S. W. Koch, Phys. Rev. B **38**, 3342 (1988).
[17] M. Kira and S. Koch, Prog. Quantum Electron. **30**, 155 (2006).
[18] H. Wang, K. Ferrio, D. G. Steel, Y. Z. Hu, R. Binder, and S. W. Koch, Phys. Rev. Lett. **71**, 1261 (1993).
[19] To account for higher correlations on the triplet level that lead to a dephasing of the doublets, we have included a phenomenological dephasing of the correlations on the order of the intraband scattering.
[20] R. Binder, S. W. Koch, M. Lindberg, N. Peyghambarian, and W. Schäfer, Phys. Rev. Lett. **65**, 899 (1990).
[21] F. Rossi and T. Kuhn, Rev. Mod. Phys. **74**, 895 (2002).
[22] T. Shih, K. Reimann, M. Woerner, T. Elsaesser, I. Waldmuller, A. Knorr, R. Hey, and K. Ploog, Phys. Rev. B **72**, 195338 (2005).
[23] T. Wolterink, V. Axt, and T. Kuhn, Phys. Rev. B **67**, 115311 (2003).